Synthesis, characterization of new carboxylic acid salts, and study of their activity as corrosion inhibitors

Muna Raad Mahmood
Department of Chemistry, College of Science, Al-Nahrain University, Jadriya, Baghdad-Iraq
munaaltaee15@gmail.com

Mehdi Salih Shihab*
Department of Chemistry, College of Science, Al-Nahrain University, Jadriya, Baghdad-Iraq
mehdi_shihab@yahoo.com

ABSTRACT

In this study, novel organic ammonium salts, 4-{[(2Z)-3-carboxyprop-2-enoyl]-amino}benzoate tetraethyl ammonium, C1, 2-[(4-carboxyphenyl)carbamoyl]-benzoate tetraethyl ammonium, C2, 4-[(3-carboxypropanoyl)amino]-benzoate tetraethyl ammonium, C3, 2-[(4-carboxyphenyl)carbamoyl]-benzoate tetraethyl ammonium, C4, and the structures have been verified using spectroscopic methods. The recently developed organic ammonium salts were used as corrosion inhibitors to protect mild steel from corrosion. The experimental procedure included putting organic salts in a 3.5% saline solution for 24 hours at room temperature. The weight-loss technique was used to assess the effects of this treatment. The findings referring to the inhibition effectiveness of organic inhibitors (C1–C4) showed an increase as the concentrations of organic ammonium salts rose. This rise in inhibition efficiency was shown to be followed by a reduction in the corrosion rate. The increased level of inhibitory efficiency resulted in a rise in the coated surface degree factor. The thermodynamic parameter, namely the free energy, was anticipated to determine the physisorption impact of several organic ammonium salts (C1–C4).

Keywords: Corrosion; Ionic Liquid; Corrosion inhibitors; Carboxylic acids

Introduction

The happenings of Corrosion is a phenomenon that takes place on the external surface or inside the interior of a metal's structure [1]. The formation of corrosion is linked to a corrosion phenomenon that occurs through an electrochemical procedure that occurs when a metal undergoes a reaction with its surrounding environment, leading to the production of an oxide or another substance [2]. A corrosion inhibiting agent is a kind of chemical liquid that is used inside a particular environment to decrease the process of corrosion that occurs to a metal that is subjected to such environments [3, 4], such as air or water [5, 6].

Carboxylic acids are a class of organic compounds that include a carboxyl functional group (-COOH). They are characterized by Salts are classified as organic compounds and may be represented by the generic formula (RCOOM), where ($RCOO^{--}$) denotes the carboxylic acid component and (M^{++}) represents the alkali component. In the context of this experiment, the alkali component may consist of a metal cation such as sodium (Na^{+}) or potassium (K^{+}), or it may be ammonium ($NH4^{++}$). The aforementioned salts exhibit the physical property of being colorless or white crystalline solids and possess the characteristic of solubility in both cold and hot water [7, 8].

Ionic liquids (ILs) are typically defined as substances consisting totally of ions and having a melting point below 100 °C [9, 10]. The first discovery of ILs, namely ethylammonium nitrate (IL), may be attributed to Paul Walden in 1914 [11]. However, at the time of his discovery, Walden wasn't prepared for the significant advances in science and widespread interest that ILs would garner over the course of almost a century. In recent years, there has been a significant increase in the attention given to innovative fluids, often referred to as ILs. The quantity of scientific articles on ionic liquids (ILs) published in SCI journals has had a significant exponential rise, starting with a small number in 1996 and surpassing 5000 in 2016 [12, 13]. This growth rate has exceeded the yearly rates of expansion observed in other prominent scientific fields. This suggests that an increasing number of scholars are actively involved in investigating this captivating field, resulting in a multitude of findings. There is a growing body of interdisciplinary research focused on ionic liquids (ILs), including several fields such as chemistry, materials science, chemical engineering, and environmental science. In light of increased understanding of the nature of ionic liquids (ILs) [14], some essential perspectives have undergone notable modifications compared to their initial conceptions. The physicochemical properties of ionic liquids (ILs) are now acknowledged to include a wide range, extending beyond the often-cited characteristics of being nonvolatile, non-flammable, and stable in air and water. Some ILs exhibit specific volatility, flammability, and instability [15].

2.0 Experimental

2.0.1 Reagents and solvents

All of the chemicals utilized in this study have been obtained from Merck and Fluka.

2.0.2 Synthesis

General method for synthesis of tetraethyl ammonium salts

The synthesized of tetraethyl ammonium salts had names: 4-{[(2Z)-3-carboxyprop-2-enoyl]-amino}benzoate tetraethyl ammonium, C1, 2-[(4-carboxyphenyl)carbamoyl]-benzoate tetraethyl ammonium, C2, 4-[(3-carboxypropanoyl)amino]-benzoate tetraethyl ammonium, C3, 2-[(4-carboxyphenyl)carbamoyl]-benzoate tetraethyl ammonium, C4. These organic ammonium salts (C1-C4) were synthesized as below:

A mixture of (0.01 mol) benzoic acid with (0.01 mol) (phthalic anhydride, maleic anhydride, succinic anhydride or glutaric anhydride) in 15 mL of THF as a solvent was stirred for four hours at room temperature to obtain amic acid compounds (B1-B4). Then left the mixture 24 hours at room temperature. The crude compound that obtained was filtered, then washed two times by 5 mL THF solvent. Then, equivalent molar of each amic acid (B1-B4) and tetraethyl ammonium hydroxide (35%) was mixed with 5 mL CH_3OH as a solvent and stirred at room temperature for 3 hours. The mixture was left for 48 hours at 37 °C. The final organic salt (C1-C4) was washed with 5 mL of methanol two times then dried [16]. The final product shown as figure 1.

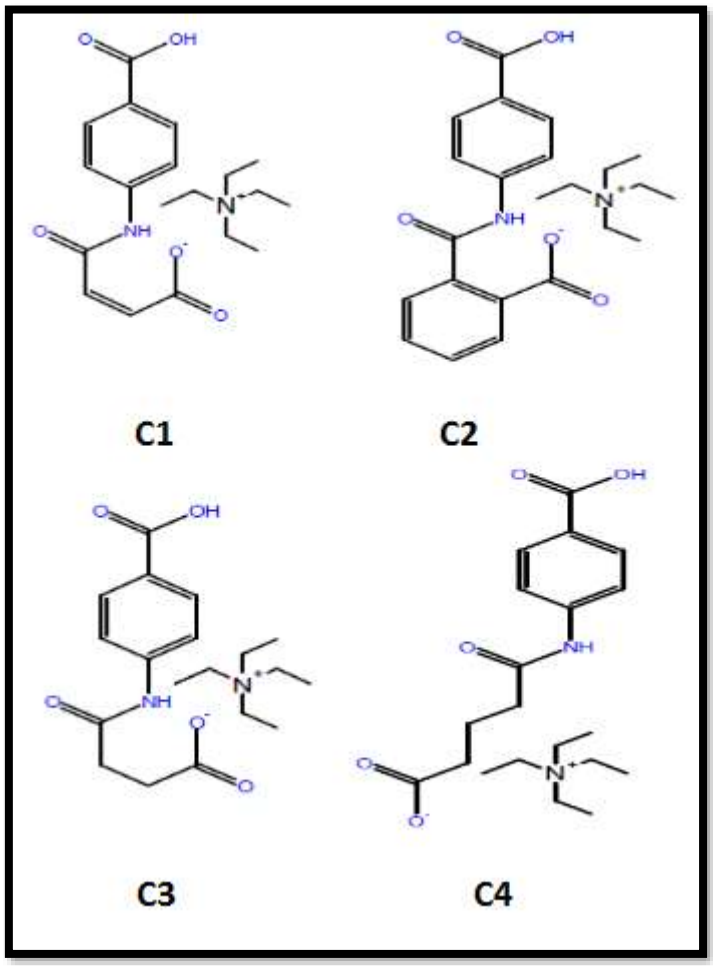

Figure 1: Chemical structure of compounds C1-C4.

B1, 4-{[(2Z)-3-carboxyprop-2-enoyl]-amino}benzoic acid, mp: 101 – 103 °C, Yield %:69, FTIR data (cm-1): N-H amide 3312, =C-H olefinic 3210, =C-H aromatic 3063, -C=O carboxylic 1716, -C=O amide 1645 [17]. As shown figure 2.

B2, 2-[(4-carboxyphenyl)carbamoyl]-benzoic acid, mp: 156 - 158°C, Yield %:77, FTIR data (cm-1): N-H amide 3302, =C-H aromatic 3060, -C=O carboxylic 1727, -C=O amide 1644. As shown figure 3.

B3, 4-[(3-carboxypropanoyl)amino]-benzoic acid, mp: 220 – 222 °C, Yield %:67, FTIR data (cm-1): N-H amide 3302, =C-H aromatic 3070, -C=O carboxylic 1722, -C=O amide 1663. As shown figure 4.

B4, 2-[(4-carboxyphenyl)carbamoyl]-benzoic acid, mp: 155-157°C, Yield %:71, FTIR data (cm-1): N-H amide 3277, =C-H aromatic 3085, -C=O carboxylic 1728, -C=O amide 1642 [18]. As shown figure 5.

C1: 4-{[(2Z)-3-carboxyprop-2-enoyl]-amino}benzoate tetraethyl ammonium, bp: 218 °C.
Yield %:76, FTIR data (cm^{-1}): -N-H amide 3231, -C-H aliphatic 2986, 2852, =C-H aromatic 3050, -C=O carboxylate 1712, -C=O amide 1641, 1H-NMR data (ppm): N^+(12H, $-CH_3$, m, 1.1; 8H, $-CH_2$, m, 3.1), unsaturated alkane (2H, d, 5.9, 6.3), aromatic ring (4H, m, 6.5-7.7), N-H amide (1H, s, 7.9), COOH (1H, s, 14.8) [19], as shown figure 6 and 10.

C2: 2-[(4-carboxyphenyl)carbamoyl]-benzoate tetraethyl ammonium, bp: 230 °C.
Yield %:73, FTIR data (cm^{-1}): -N-H amide 3250, =C-H aromatic 3071, -C=O carboxylate 1718, -C=O amide 1668, as shown figure 8. 1H-NMR data (ppm): N^+(12H, $-CH_3$, m, 1.1; 8H, $-CH_2$, m, 3.1), aromatic ring (8H, m, 6.5-7.8), N-H amide (1H, s, 8.2), COOH (1H, s, 14.2), as shown figure 7 and 11.

C3: 4-[(3-carboxypropanoyl)amino]-benzoate tetraethyl ammonium, bp: 177 °C. Yield %:74, FTIR data (cm^{-1}): -N-H amide 3224, -C-H aliphatic 2987, 2870, =C-H aromatic 3057, -C=O carboxylate 1720, -C=O amide 1658, 1H-NMR data (ppm): N^+(12H, $-CH_3$, m, 1.1; 8H, $-CH_2$, m, 3.1), alkane group (4H, m, 2.2-2.7), aromatic ring (4H, m, 6.5-7.8), N-H amide (1H, s, 10.5), as shown figure 8 and 12.

C4: 2-[(4-carboxyphenyl)carbamoyl]-benzoate tetraethyl ammonium, 219 °C.

Yield %:75, FTIR data (cm^{-1}): -N-H amide 3212, -C-H aliphatic 2984, 2875, =C-H aromatic 3058, -C=O carboxylate 1710, -C=O amide 1644, 1H-NMR data (ppm): N^+(12H, $-CH_3$, m, 1.1; 8H, $-CH_2$, m, 3.1), alkane group (6H, m, 2.1-2.2), aromatic ring (4H, m, 6.5-7.9), N-H amide (1H, s, 8.2), -COOH (1H, s, 13.3), as shown figure 9 and 13.

Preparation of aggressive solution

Analytical grade NaCl with distilled water was dissolved to yield an aggressive solution of 3.5% saline solution. The inhibitor concentrations in between ($5x10^{-4}$ – $1x10^{-2}$ M) were achieved with 3.5% saline solution.

Weight loss measurements

The composition of the mild steel specimen includes the following elements: 0.002% phosphorus (P), vanadium (V), and molybdenum (Mo), 0.03% carbon (C), 0.0154% sulfur (S), 0.288% manganese (Mn), 0.065% copper (Cu), 0.0199% chromium (Cr), and 0.0005% of other elements, with the remaining element being iron (Fe). The mild steel sheet was transformed into a circular shape resembling a disk, with a diameter of 2.5 cm. The disc forms underwent surface treatment to achieve a smooth texture, using several grades of emery paper. Subsequently, the specimens with flat surfaces received a complete washing process, first with distilled water, followed by alcohol, and ultimately with acetone. The recently cleaned samples have been carefully arranged inside a suitable desiccator equipped with a drying agent. To begin the weight reduction procedure, the specimen disc is first positioned on the electronic scale to establish its weight. The second stage involves submerging the specimen disc entirely in an appropriate vessel filled with a saline solution of 3.5% concentration. This is done both in the absence and presence of an organic inhibitor of known concentration. Subsequently, the content vessel is allowed to remain undisturbed for a duration of 24 hours at ambient temperature conditions. Subsequently, the specimen disc is extracted and subjected to a cleaning process including distilled water, followed by acetone. The specimen disc undergoes reweighting once again. The weight reduction experiment was conducted in accordance with the ASTM investigation [20]. The weight reduction experiment was replicated twice in order to get the mean value. The loss of weight test findings were utilized to ascertain the mean corrosion rate ($mg.cm^{-}2.h^{-1}$). The formula (1) [21] may be used to determine the average rate of corrosion for mild steel testing.

$$W=\Delta m/St \quad \text{.....(1)}$$

Where W = corrosion rate ($mg\ cm^{-2}\ h^{-1}$), Δm = weight loss difference (mg) before and after specimen immersion, S = area of specimen (cm^2) and t = time of immersion (hrs).

The inhibition efficiency (IE%) could be calculated by using the formula (2):

$$IE\%=(W_{corr}-W_{(corr(inh))})/W_{corr}\ x100 \quad \text{.....(2)}$$

3. Results and discussions

3.1. Experimental Investigation

The preparation of tetraethylammonium salts (C1-C4) of the present work were involved synthesis of the amic acid compounds (B1-B4) by using isonicotinic acid hydrazide by reacting with a proper acid anhydride. Then the amic acids achieved a reaction of acid-base with tetraethylammonium hydroxide to prepare tetraethylammonium salt compounds (C1-C4). The spectral data of FT-IR, as well as, physical properties of synthesized compounds (B1-B4 and C1-C4) and the 1H-NMR spectral data were shown for tetraethylammonium salts (C1-C4).

3.2. Corrosion investigation

The deterioration of mild steel was determined at room temperature and after 24 hrs immersing in 3.5% aqueous NaCl solution.

The results of (corrosion rate and inhibition efficiency) were determined by using the tests of weight loss measurements with different concentrations of tetraethylammonium salts (C1-C4) that are shown in Table 1.

The findings shown in Table 1 show a positive correlation between the concentration of inhibitor (C1-C4) and the level of inhibition. Specifically, it is seen that the maximum levels of inhibition efficiency are achieved at a concentration of 0.01 M. The comparative order of inhibitory effectiveness would be as follows: C2 exhibits the highest inhibition efficiency, followed by C4, C1, and C3 [14]. These values signal the level at which the adsorption process of organic inhibitor molecules onto the surface of mild steel is successful. The fundamental principles below the adsorption could clarify the natural interaction between organic inhibitor molecules and metal surfaces. Hence, the determination of the covering surface degree, designated as θ, at various inhibitor doses was conducted using the weight loss technique in the presence of a 3.5% aqueous NaCl solution (θ = IE(%)/100) as shown in Table 1, at ambient temperature conditions [22].

The findings shown in Table 1 show a positive correlation between the concentration of inhibitors (B1–B4) and the efficiency of inhibition. Specifically, it is seen that the best efficiencies of inhibition are achieved at a concentration of 0.01 M. The relative order of inhibitory efficiency, as determined by the experimental results, is C2>C4>C1>C3. The impact of molecular organic structures, namely those with flexible structures including C2 and stiff structures containing C1, C2, and C3, on inhibition efficiency might potentially be elucidated by examining the values of inhibition efficiency [23]. These values indicate the extent to which organic inhibitor molecules are able to successfully undergo the adsorption process on the surface of mild steel. The technique of adsorption may provide fundamental information on the elutriation process and the inherent interaction between organic inhibitor molecules and metal surfaces. Hence, the determination of the coverage surface degree, denoted as θ, at various inhibitor doses was conducted using the weight loss technique in the presence of a 3.5% aqueous NaCl solution. The coverage surface degree (θ) was calculated as the ratio of the inhibitor efficiency (IE) expressed as a percentage to 100. The experimental conditions and results are shown in Table 1, and the experiments were carried out at room temperature [22]:

$$C/\theta = 1/K_{ads} + C \quad \ldots\ldots\ldots\ldots (3)$$

Where: C (concentration, M), Kads, equilibrium constant of adsorption process (M-1).

By applying the Langmuir isotherm, that value Kads is estimated from straight line intersection of C versus C/θ. The values of ΔG^{o}_{ads} was determined by equation (4) [22]: (55.5 value: water molar concentrations, M).

$$K_{ads} = 1/55.5 \exp(-(\Delta G^{o}_{ads})/RT) \quad \ldots\ldots\ldots\ldots (4)$$

Table 1 displays the free energy values associated with the adsorption process, indicating a negative sign. This signifies that the adsorption processes for compounds C1-C4 occur spontaneously on the surface of mild steel when immersed in a 3.5% aqueous NaCl solution at room temperature for a duration of 24 hours. These findings provide evidence of the effective interaction between the organic molecules C1-C4 and the metal surface. Furthermore, it is possible to transport organic inhibitor molecules towards the metal surface and bring them into proximity, therefore disrupting the electron interactions between the organic molecules and the vacant atomic orbitals on the metal surface [24]. Additionally, this interference may also disrupt the retro-donation process [25]. The adsorption phenomenon of organic inhibitor molecules onto the surface of a metal may be attributed to the creation of a complexation between the organic inhibitor molecules and the metal surface, as shown by Equations (5) and (6) below:

$$Fe + xH_2O \rightarrow Fe(H2O_{ads})x \quad \ldots\ldots\ldots\ldots\ldots (5)$$

$$Fe(H2O_{ads})x + Inh_{sol} \rightarrow \text{Fe-Inh complex} + xH2O \quad \ldots\ldots\ldots\ldots (6)$$

$Fe\ (sold) + 2H^{+} \rightarrow Fe^{+2}(solution) + H_2$ .....(7)

$O_2\ (g) + 2H_2O + 4e^{-} \rightarrow 4OH^{-}$ .....(8)

As a result, the metal-inhibitor complex has the capability to function as a thin layer film on the anode sites, therefore mitigating or inhibiting the production of Fe2+ ions (refer to Equations 7 and 8). It is noteworthy to notice that the quantity of metal-inhibitor complexes present on the metal surface decreases as the concentration of organic inhibitors decreases. The adsorption process of inhibitor molecules is elucidated by the effective interaction of organic molecules with the electrons of nitrogen and oxygen atoms present in the organic molecular inhibitors. According to reports, the adsorption process may be influenced by the presence of functional groups inside the structural molecule, which in turn can alter the electron density of the molecule. The adsorption of organic inhibitor salts (C1-C4) onto the surface of mild steel results in the creation of a thin layer complex. This complex effectively blocks the active sites of the anode, hence preventing or reducing the electrochemical dissolution reaction that leads to the loss of metal atoms from the surface of the steel.

Table 1. Rate of corrosion, inhibition efficiency (IE%), surface coverage (θ) and $\Delta G°_{ads}$ for test of mild steel in 3.5% aqueous NaCl solution with weight loss method for 24 hrs and at room temperature.

Concentration (M)	Corrosion rate (mg.cm^{-2}.h^{-1})	Θ	IE%	$\Delta G°_{ads}$ (kJ. mol^{-1})
Blank	0.3440			
C1				
1×10^{-2}	0.0081	0.8333	83.33	-29.30
5×10^{-3}	0.0098	0.7984	79.84	
1×10^{-3}	0.0115	0.7633	76.33	(R^2=0.9996)
5×10^{-4}	0.0132	0.7284	72.84	
C2				
1×10^{-2}	0.0081	0.9609	96.09	-30.99
5×10^{-3}	0.0085	0.9588	95.88	
1×10^{-3}	0.0102	0.7901	79.01	(R^2=0.9998)
5×10^{-4}	0.0144	0.7037	70.37	
C3				
1×10^{-2}	0.0098	0.7984	79.84	-31.53
5×10^{-3}	0.0110	0.7737	77.37	
1×10^{-3}	0.0136	0.7202	72.02	(R^2=0.9998)
5×10^{-4}	0.0162	0.6667	66.67	
C4				
1×10^{-2}	0.0064	0.8683	86.83	-30.85
5×10^{-3}	0.0089	0.8169	81.69	
1×10^{-3}	0.0115	0.7633	76.33	(R^2=0.9983)
5×10^{-4}	0.0132	0.7284	72.84	

Conclusion

The synthesis of tetraethyl ammonium organic salts (C1– C4) was successfully completed as a method of producing corrosion organic molecules that inhibit corrosion for the purpose of protecting mild steel surfaces. This synthesis process took place in a solution of aqueous saline at room temperature for a duration of 24 hours. The findings of this study demonstrated significant inhibitory effects of the tetraethyl ammonium organic salts that were synthesized, as shown by the efficiency inhibition (IE%) values. The free energy adsorption values were determined for the

physical process of adsorption (C1, C2, C3, and C4) and provided significant data to elucidate the inherent interaction between the organic inhibitor molecules and the mild steel surface.

Acknowledgment

The authors are being thankful to the Department of Chemistry at Al-Nahrain University, Iraq, for their cooperation and help throughout this work.

References

1. Hersbach, T.J. and M.T. Koper, *Cathodic corrosion: 21st century insights into a 19th century phenomenon.* Current Opinion in Electrochemistry, 2021. **26**: p. 100653.
2. Czaban, M., *Aircraft corrosion–review of corrosion processes and its effects in selected cases.* Fatigue of Aircraft Structures, 2018. **2018**(10): p. 5-20.
3. Kadhim, A., et al., *Corrosion inhibitors. A review.* International Journal of Corrosion and Scale Inhibition, 2021. **10**(1): p. 54-67.
4. Alrefaee, S.H., et al., *Challenges and advantages of using plant extract as inhibitors in modern corrosion inhibition systems: Recent advancements.* Journal of Molecular Liquids, 2021. **321**: p. 114666.
5. Pan, C., X. Li, and J. Mao, *The effect of a corrosion inhibitor on the rehabilitation of reinforced concrete containing sea sand and seawater.* Materials, 2020. **13**(6): p. 1480.
6. Pareek, S., et al., *A review on inhibitors alleviating copper corrosion in hostile simulated sea-water (3.5 wt.% NaCl solution).* Materials Today: Proceedings, 2021. **43**: p. 3303-3308.
7. Ahamad, M.N., et al., *Metal organic frameworks decorated with free carboxylic acid groups: topology, metal capture and dye adsorption properties.* Dalton Transactions, 2020. **49**(41): p. 14690-14705.
8. Smith, M.B., *Biochemistry: an organic chemistry approach*. 2020: CRC Press.
9. Kaur, G., H. Kumar, and M. Singla, *Diverse applications of ionic liquids: A comprehensive review.* Journal of Molecular Liquids, 2022. **351**: p. 118556.
10. Buettner, C.S., et al., *Surface-active ionic liquids: A review.* Journal of Molecular Liquids, 2022. **347**: p. 118160.
11. Reddy, A.V.B., et al., *Introduction to ionic liquids and their environment-friendly applications*, in *Ionic Liquid-Based Technologies for Environmental Sustainability*. 2022, Elsevier. p. 1-15.
12. Lei, Z., et al., *Introduction: ionic liquids*. 2017, ACS Publications. p. 6633-6635.
13. Vereshchagin, A.N., et al., *Quaternary ammonium compounds (QACs) and ionic liquids (ILs) as biocides: from simple antiseptics to tunable antimicrobials.* International journal of molecular sciences, 2021. **22**(13): p. 6793.
14. Hayes, R., G.G. Warr, and R. Atkin, *Structure and nanostructure in ionic liquids.* Chemical reviews, 2015. **115**(13): p. 6357-6426.
15. Rosini, S.B., *Ionic Liquids for Application in Separation Processes: Chromatographic and Calorimetric Studies*. 2018, Instituto Politecnico de Braganca (Portugal).
16. Baboian, R., *Corrosion tests and standards: application and interpretation*. Vol. 20. 2005: ASTM international.
17. Berthomieu, C. and R. Hienerwadel, *Fourier transform infrared (FTIR) spectroscopy.* Photosynthesis research, 2009. **101**: p. 157-170.
18. Mohamed, M.A., et al., *Fourier transform infrared (FTIR) spectroscopy*, in *Membrane characterization*. 2017, Elsevier. p. 3-29.
19. Emwas, A.-H., et al., *NMR spectroscopy for metabolomics research.* Metabolites, 2019. **9**(7): p. 123.
20. Bai, Y., A. Chaudhari, and H. Wang, *Investigation on the microstructure and machinability of ASTM A131 steel manufactured by directed energy deposition.* Journal of Materials

Processing Technology, 2020. **276**: p. 116410.
21. Zhao, Q., et al., *Chitosan derivatives as green corrosion inhibitors for P110 steel in a carbon dioxide environment.* Colloids and Surfaces B: Biointerfaces, 2020. **194**: p. 111150.
22. Ogunleye, O., et al., *Green corrosion inhibition and adsorption characteristics of Luffa cylindrica leaf extract on mild steel in hydrochloric acid environment.* Heliyon, 2020. **6**(1).
23. Chauhan, D.S., C. Verma, and M. Quraishi, *Molecular structural aspects of organic corrosion inhibitors: Experimental and computational insights.* Journal of Molecular Structure, 2021. **1227**: p. 129374.
24. Rodríguez, J.A., et al., *Mathematical models generated for the prediction of corrosion inhibition using different theoretical chemistry simulations.* Materials, 2020. **13**(24): p. 5656.
25. Verma, C., M. Quraishi, and A. Singh, *A thermodynamical, electrochemical, theoretical and surface investigation of diheteroaryl thioethers as effective corrosion inhibitors for mild steel in 1 M HCl.* Journal of the Taiwan Institute of Chemical Engineers, 2016. **58**: p. 127-140.

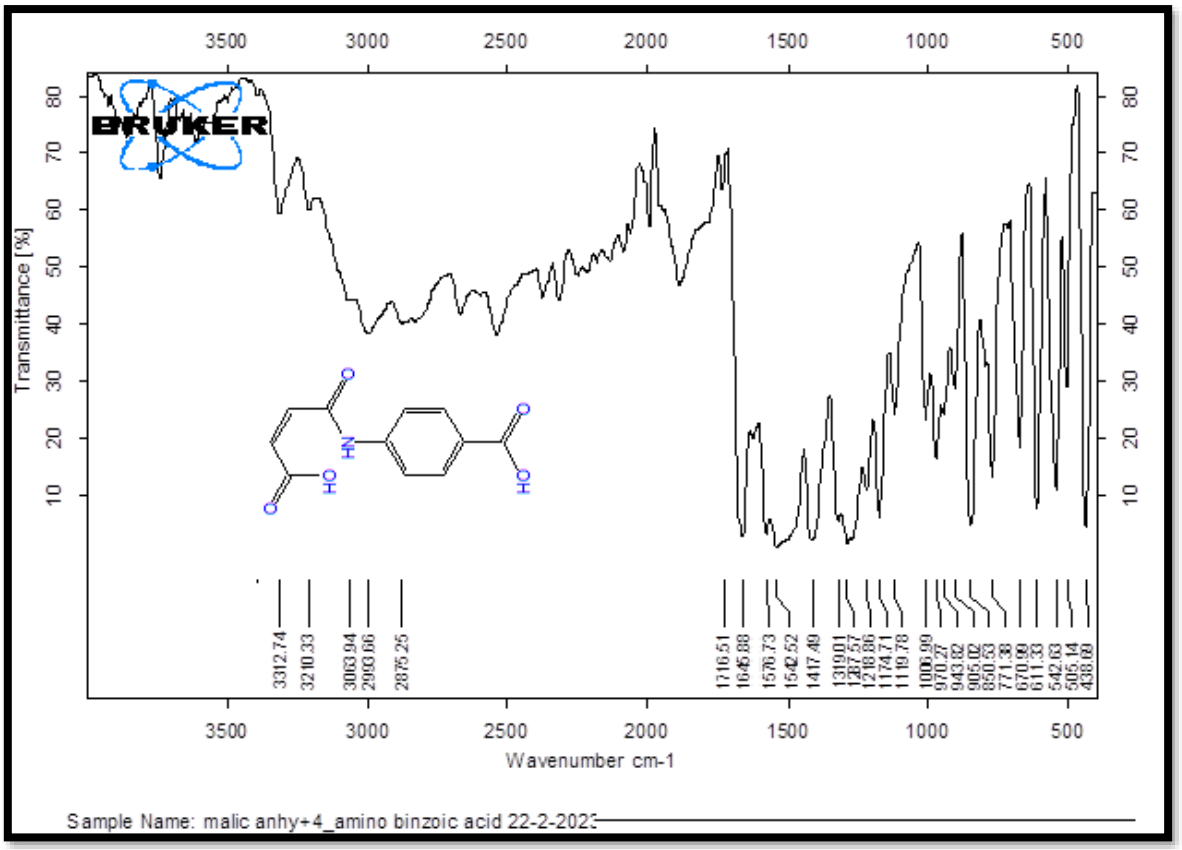

Figure 2: FTIR spectrum for compound B1.

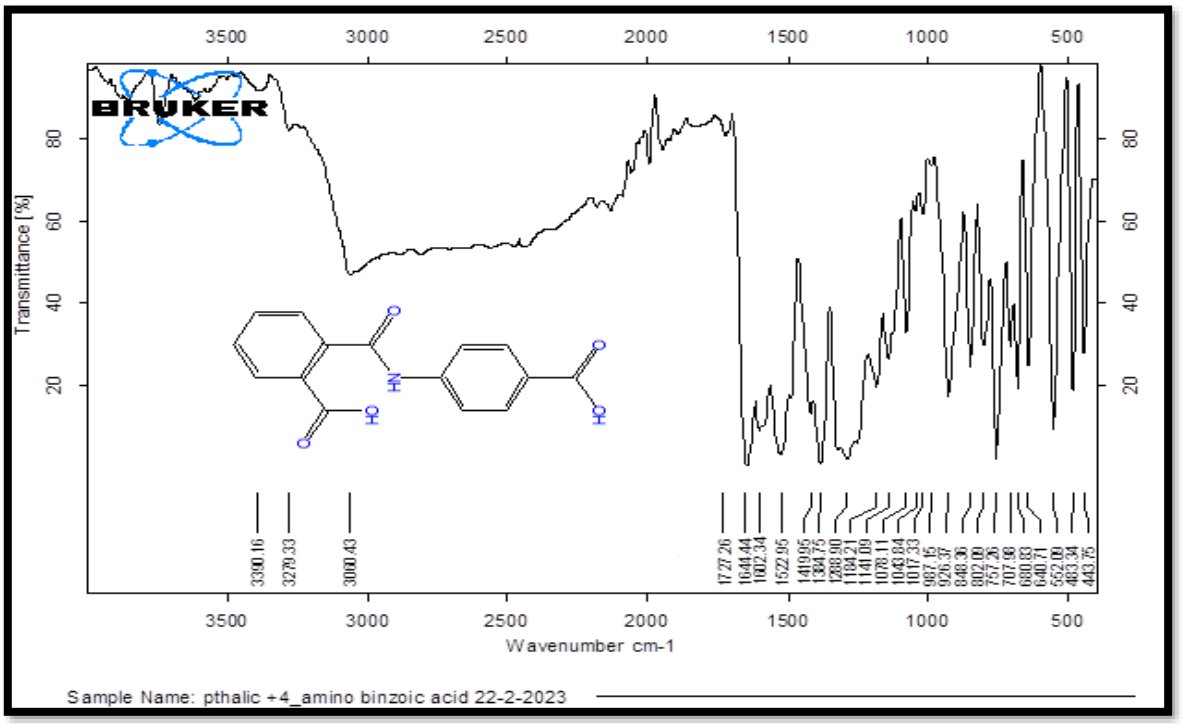

Figure 3: FTIR spectrum for compound B2.

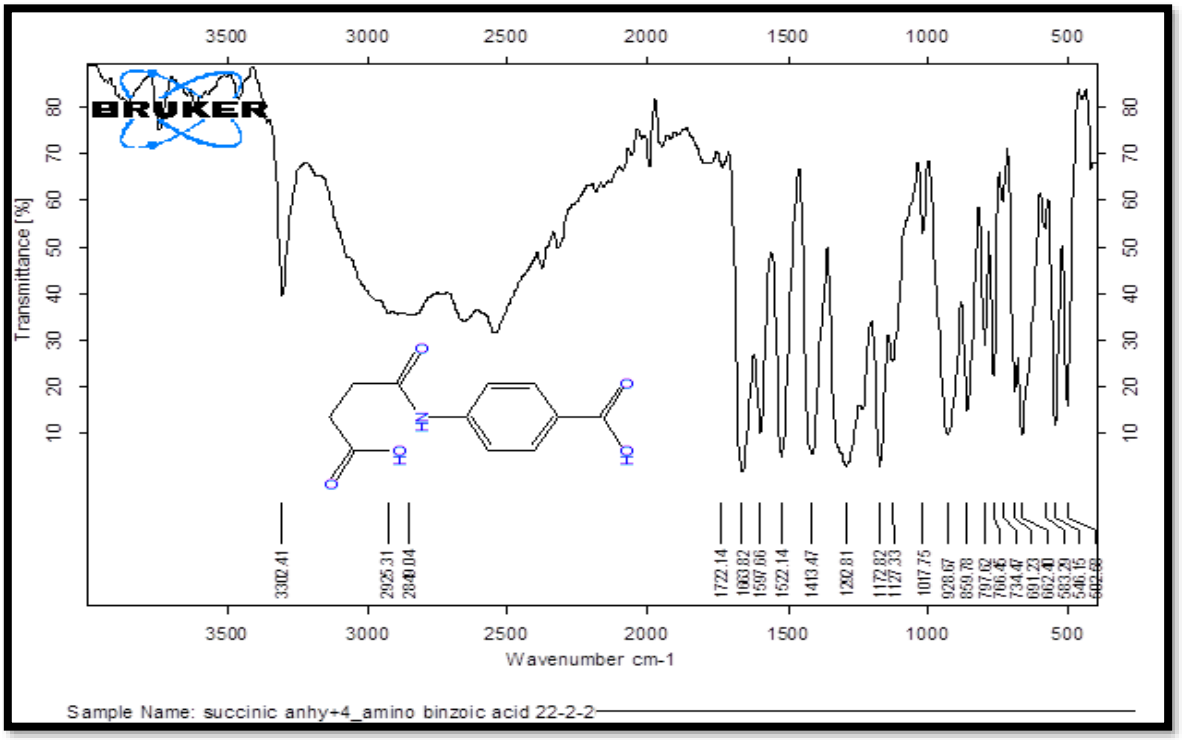

Figure 4: FTIR spectrum for compound B3.

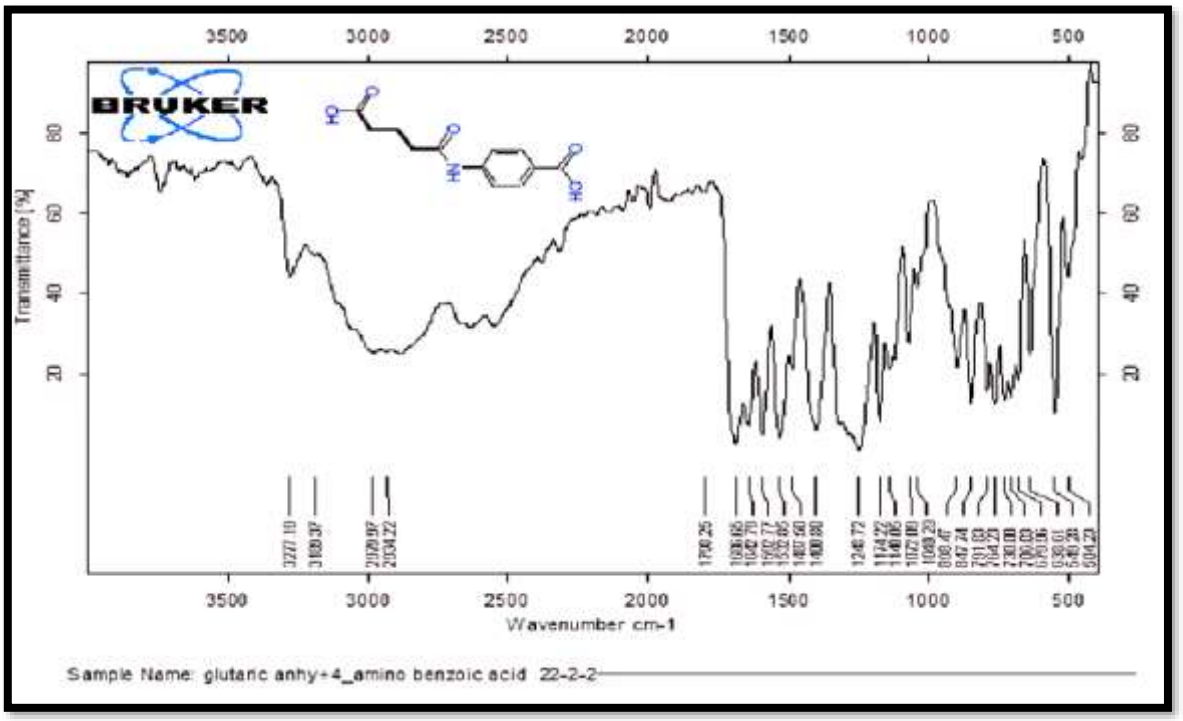

Figure 5: FTIR spectrum for compound B4.

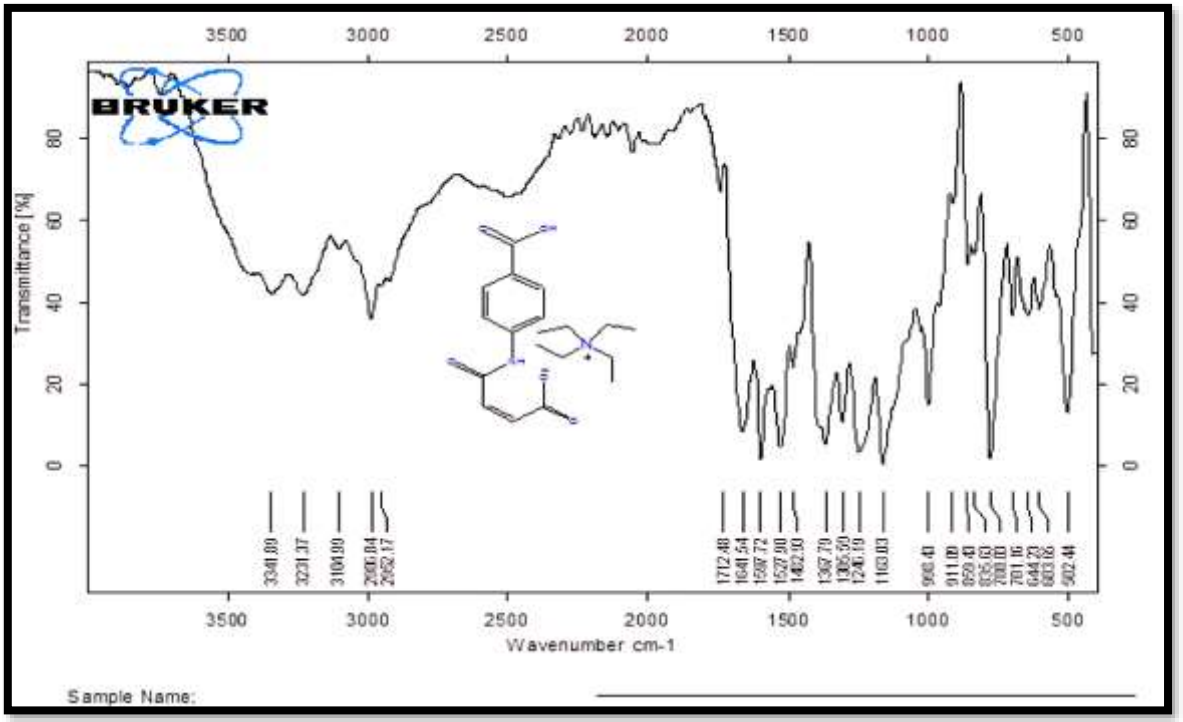

Figure 6: FTIR spectrum for compound C1.

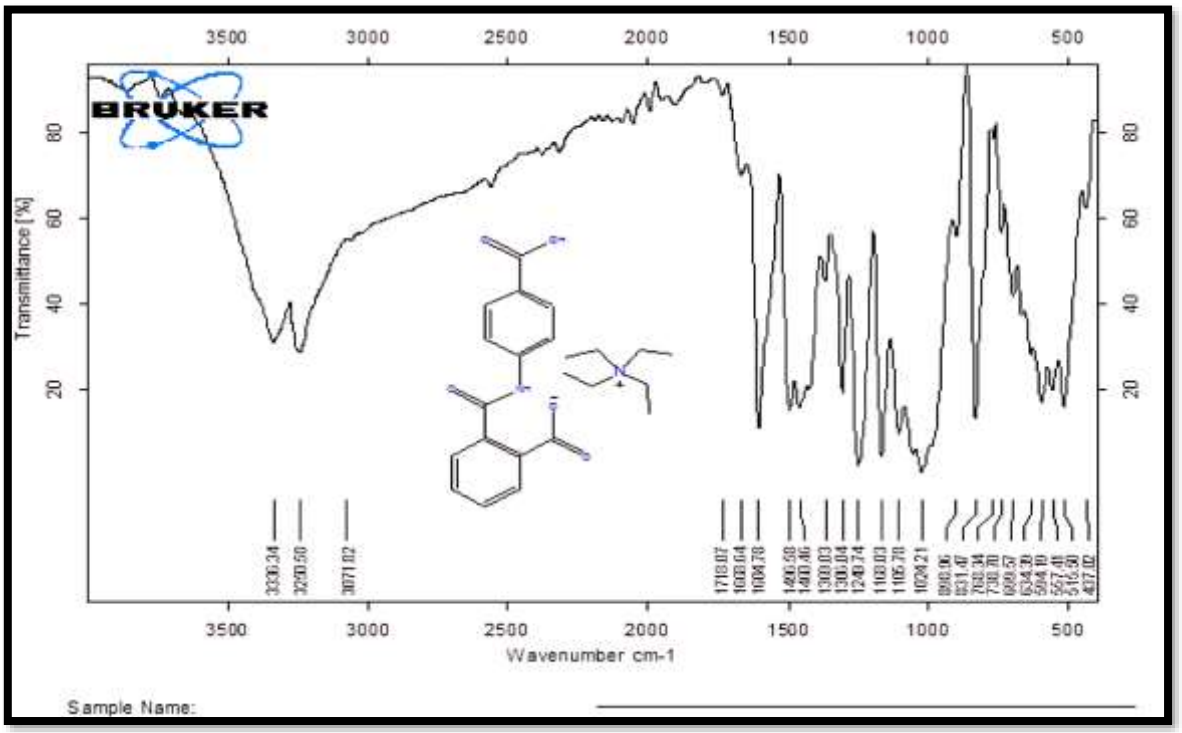

Figure 7: FTIR spectrum for compound C2.

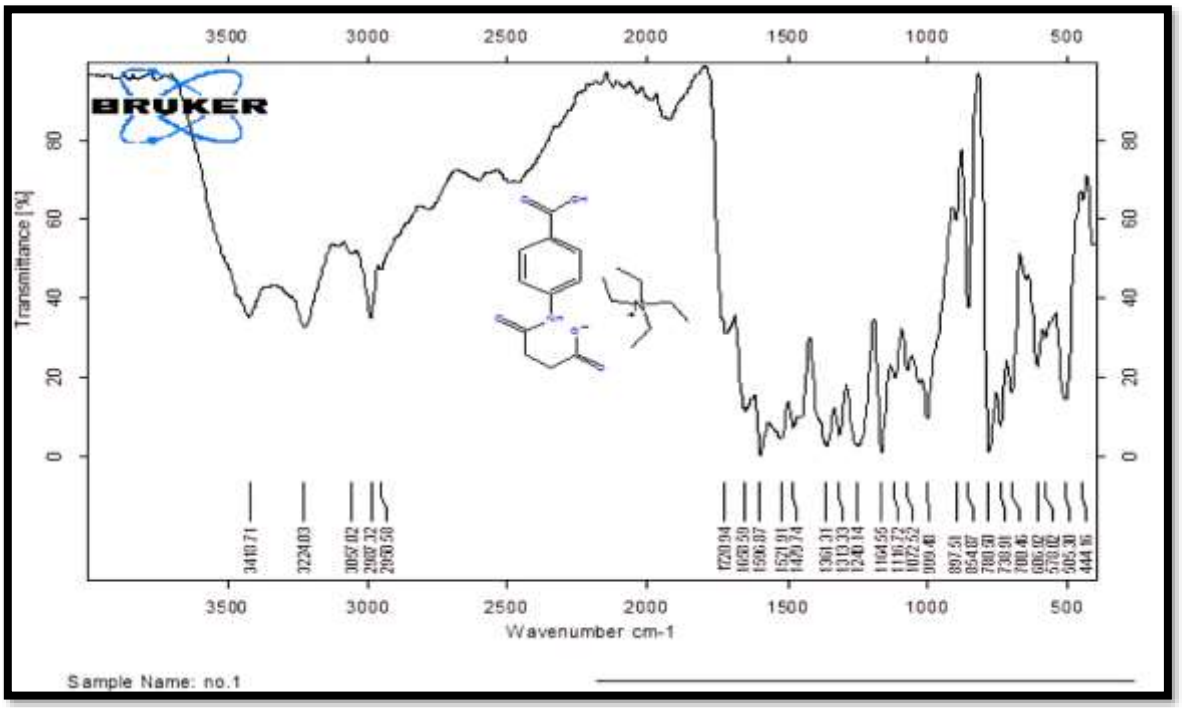

Figure 8: FTIR spectrum for compound C3.

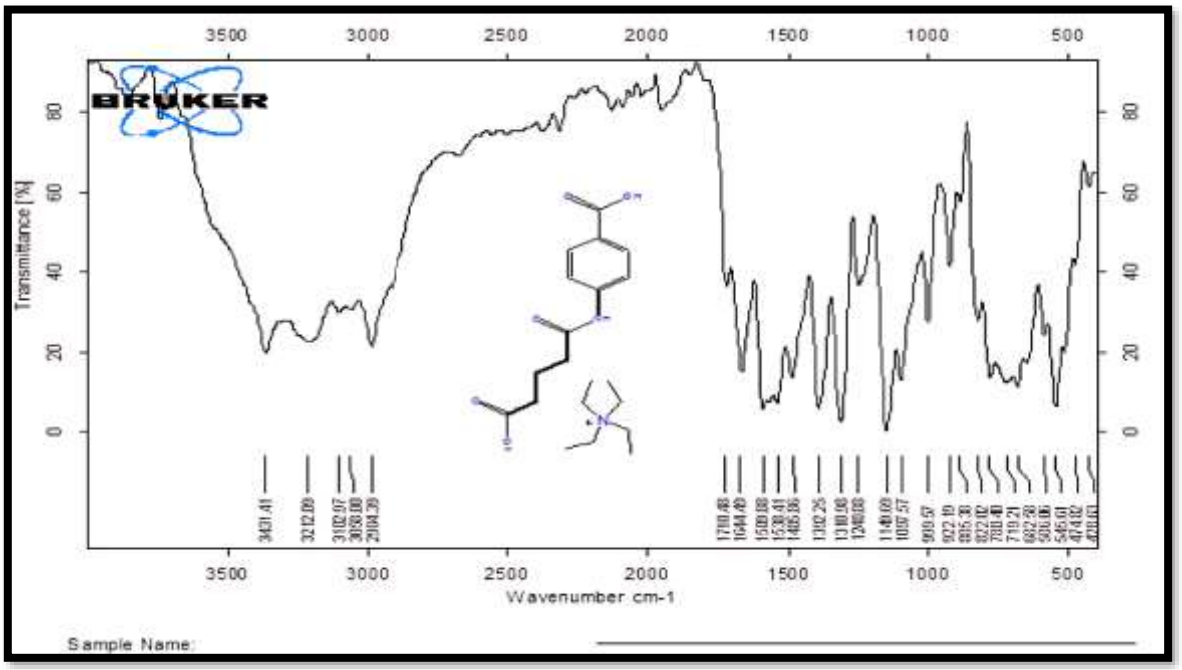

Figure 9: FTIR spectrum for compound C4.

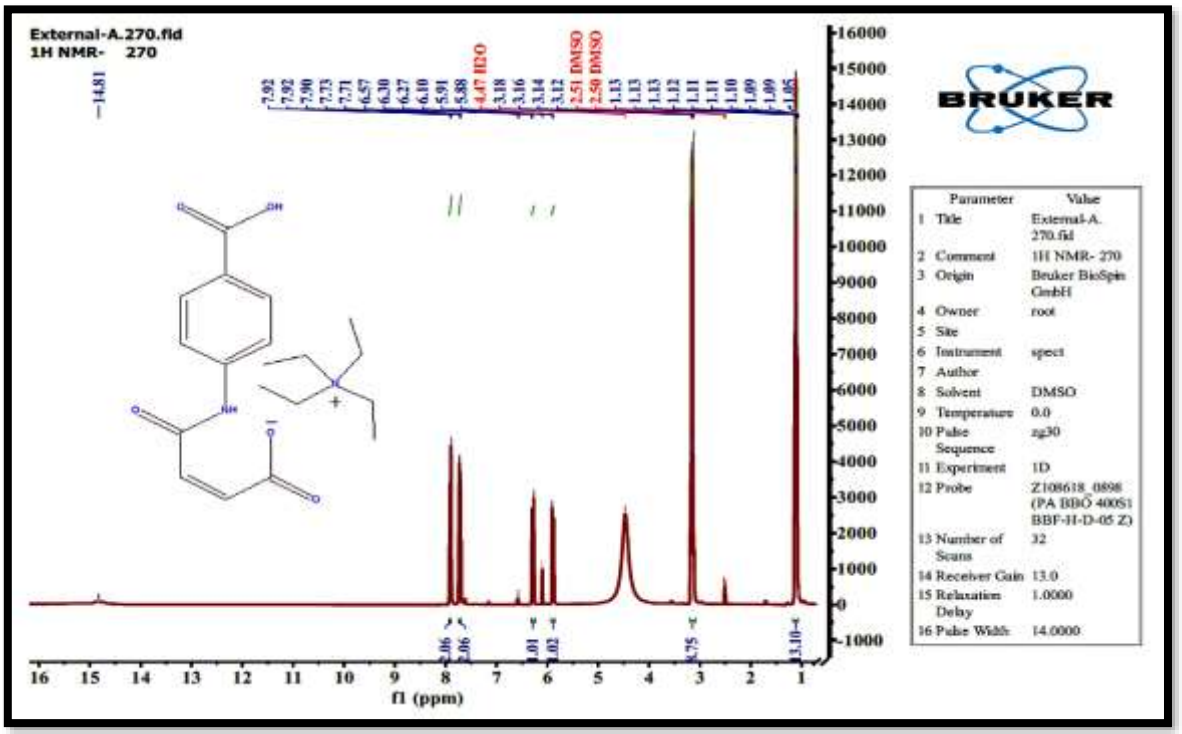

Figure 10: [1]HNMR spectrum of compound C1.

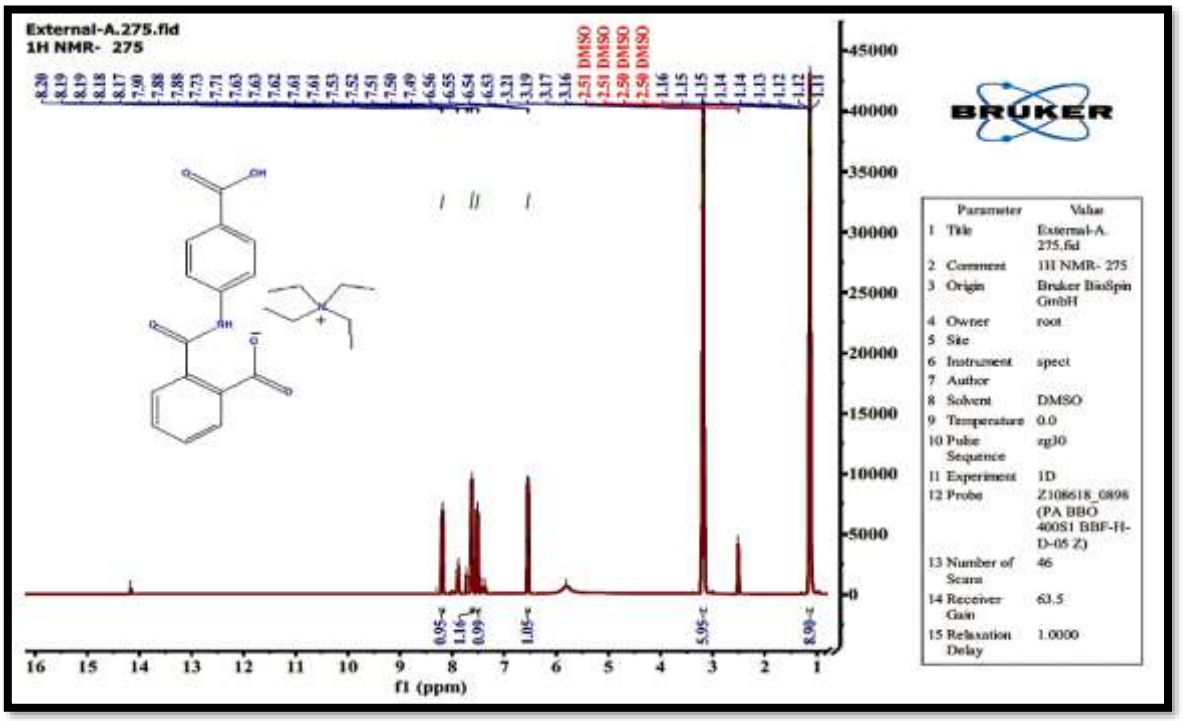

Figure 11: [1]HNMR spectrum of compound C2.

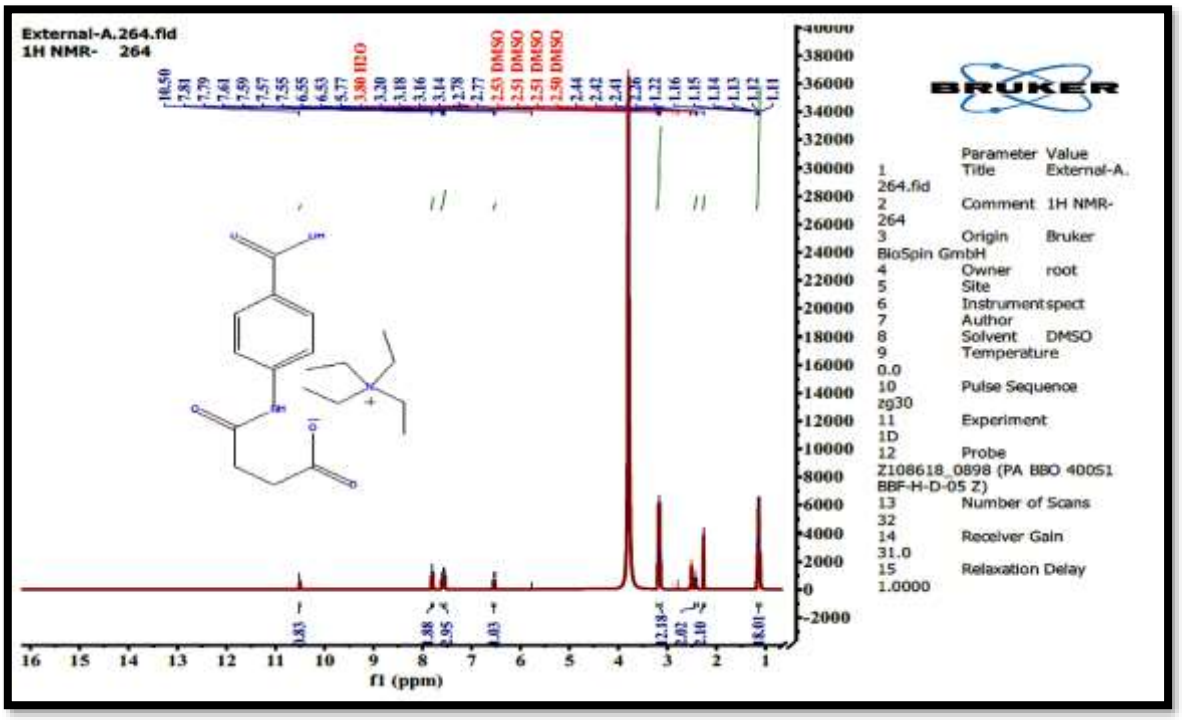

Figure 12: [1]HNMR spectrum of compound C3.

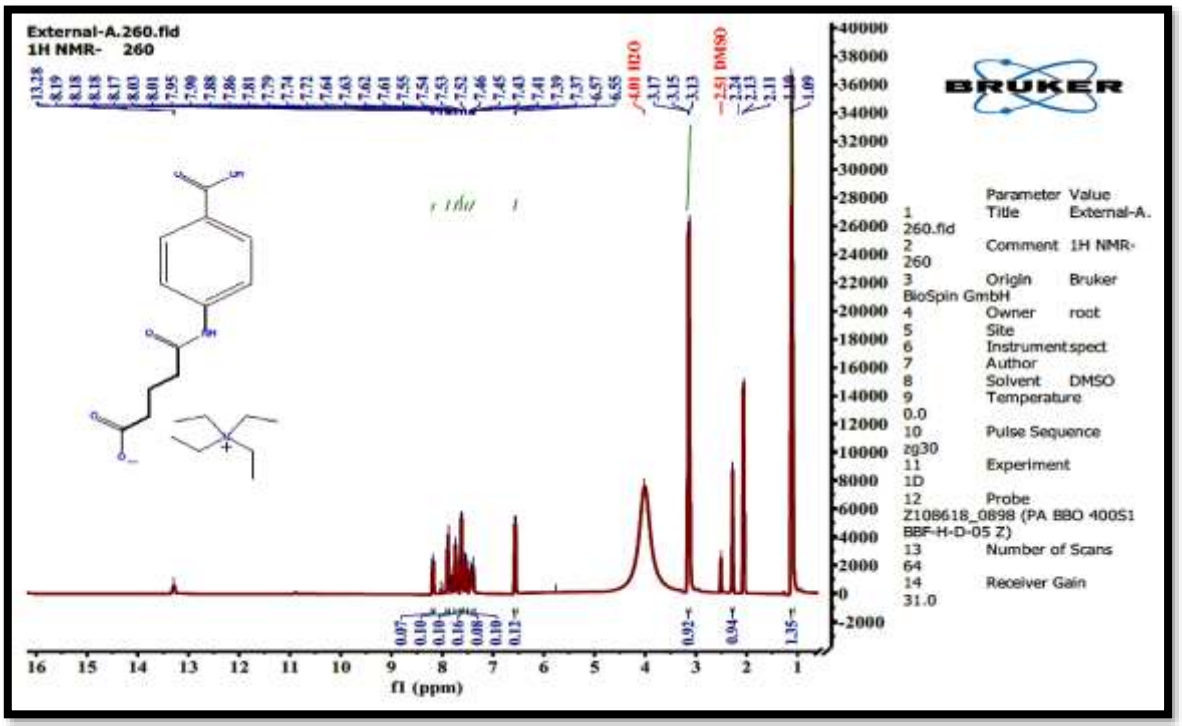

Figure 13: ^{1}HNMR spectrum of compound C4.